J Fluoresc (2012) 22:223–238
DOI 10.1007/s10895-011-0949-5

ORIGINAL PAPER

New Luminescent Bioprobes Eu(lll)-phloroglucinol Derivatives and Their Spectrofluorimetric, Electrochemical Interactions with Nucleotides and DNA

Hassan Ahmed Azab · Zeinab M. Anwar · Enas T. Abdel-Salam · Mahmoud EL-Sayed-Sebak

Received: 14 June 2011 / Accepted: 7 August 2011 / Published online: 2 September 2011

Abstract Two new ligands derived from phloroglucinol 2-{[(4-methoxy benzoyl) oxy] } methyl benzoic acid[L1] and 2-{[(4-methyl benzoyl)oxy] methyl} benzoic acid[L2] were synthesized. The solid complex Eu(III)-L2 has been synthesised and characterized by elemental analysis ,UV and IR spectra. The reaction of Eu(III) with the two synthesized ligands has been investigated in I=0.1 mol dm^{-3} p-toluene sulfonate by cyclic voltammetry and square wave voltammetry. The reaction of Eu (III)–L1 and Eu (III)–L2 binary complexes with nucleotide 5′-AMP , 5′-ADP ,5′-ATP , 5′- GMP , 5′-IMP , and 5′-CMP has been investigated using UV, fluorescence and electrochemical methods. The experimental conditions were selected such that self-association of the nucleotides and their complexes was negligibly small, that is, the monomeric complexes were studied. The interaction of the Eu(III)–L1 or L 2 solid complexes with calf-thymus DNA has been investigated by fluorescence and electrochemical methods including cyclic voltammetery(CV) ,differential pulse polarography (DPP) and square wave voltammetry (SWV) on a glassy carbon electrode. The fluorescence intensity of Eu(III)-L2 complex was enhanced with the addition of DNA. Under optimal conditions in phosphate buffer pH 7.0 at 25 °C the linear range is 3–20 μM for calf thymus DNA (CT–DNA) and the corresponding determination limit is 1.8 μM.

Keywords Fluorescence · Electrochemical probing · Nucleotides · DNA · Eu (lll)- phloroglucinol derivatives

H. A. Azab (✉) · Z. M. Anwar · E. T. Abdel-Salam · M. EL-Sayed-Sebak
Chemistry Department, Faculty of Science,
Suez Canal University,
Ismailia 41522, Egypt
e-mail: azab2@yahoo.com

Introduction

Phloroglucinol (C6H6O3, 1,3,5- trihydroxy benzene) is a starting of the production of several medicine [1] and is the parent compound of a high number of derivatives collectively called phloroglucinol most of which show biological activity and are present in a variety of natural materials utilized in traditional medicine in various continents[2–13]. Phloroglucinol is used in estimation of formaldehyde in food stuff [14] and in the manufacture of bone cement, which is biodegradable so that it doesn`t act as barrier to bone remodeling or fracture heating [15] . Phloroglucinol can be used for simultaneous determination of nitrite and nitrate in water samples which have harmful impact on human health [16] .Phloroglucinol is used as a smooth muscle relaxant ,it has no anticholinergia potency and appears to be less toxic than most other antispasmodic agents[17] .

In the last decades many rare earth metal complexes have attracted much attention due to their long fluorescence lifetimes and strong fluorescence emissions. These complexes have been used in many areas, such as fluorescence materials [18–20], electroluminescence devices [21–24] and as fluorescence probes and labels in a variety of biological systems [25–28]. Among these studies, the luminescence properties of rare earth complexes are of special interest because these complexes could show narrow emission bands, a large Stokes' shift and long luminescence decay time. The intra-configuration 4f–4f transitions in rare earth ions are parity forbidden (Laporte rule), consequently the absorption and emission spectra of the RE (III) ions show weak intensity. However, the population of the excited states of the RE (III) ions may be increased by coordination to organic ligands, which act as sensitizers [29].

The ligands that present this property were called by Lehn [30] as "antennas". In RE (III)-complex, the organic ligand absorbs and transfers energy efficiently to the metal ion (intra-molecular energy transfer) and consequently increases its luminescence intensity. So based on the different ligands and the central RE (III), many fluorescent complexes have been synthesized. The main ligands include aromatic carboxylic acid, 1-10-phenanthroline (phen), pyridine and diketone [31–33]. Lanthanide complexes with these ligands are nowadays gaining wide acceptance in the scientific community.

Here, chemosensors for specific molecules can be made using optical transduction through these ligands capturing the analyte.

The use of lanthanide ligand complexes as chromophores and recognition units can improve selectivity due to selective complex formation with the analyte. The binding event is monitored by the change of the emission of the so-called hypersensitive emission bands of the lanthanide. The emission of these bands is much more sensitive to changes of the binding partners in the primary and even in the secondary coordination sphere than emission of organic fluorophores. Luminescence decay time does not depend on ionic strength, excitation intensity and concentration of lanthanide ligand complexes sensor which makes it a more reliable parameter that is additionally an intrinsic value. This means that it is a parameter independent of the device it is detected with. The lifetime of emission from the excited state of the lanthanide ions falls in the range of microseconds (e.g. Yb and Nd) to milliseconds (e.g. Eu and Tb). Such relatively long-lived emission is an attractive feature from an analytical point of view, as it allows the implementation of time-gating procedures so that the lanthanide luminescence is readily distinguished from the shorterlived nanosecond-background present in most real samples.

Detection of specific DNA sequence is central to modern molecular biology and also to molecular diagnostics where identification of a particular disease is based on nucleic acid identification [33, 34]. The fluorescence spectroscopy dominates the detection technologies for DNA because fluorescence offers many advantages in terms of sensitivity and ease of use [35–39]. Current fluorescence detections of DNA hybridization focus on the design of a single-stranded DNA (ssDNA) labeled with a dye-quencher pair (molecular beacons) [40, 41]. However, the approaches require the dye-quencher pair optimization, sophisticated probe design and synthesis.

In this work, we observed the interesting phenomenon that if CT–DNA was added into Eu (III)-phloroglucinol derivatives solutions, the CT–DNA–Eu (III)- phloroglucinol derivatives systems can produce the strong fluorescence emission.

By taking advantage of this phenomenon, a new strategy for CT–DNA hybridization can be suggested using Eu (III)-phloroglucinol derivatives as fluorescence probe. Furthermore, this label-free method for CT–DNA hybridization detection can avoid the laborious labeling or modifying steps, which can make the process simple, rapid, and low in cost; the hybridization and detection are performed in homogeneous solution without steric constraints. Herein, the aim of the present study is to examine the interaction of Eu(III) with two synthesized phloroglucinol derivatives (2-{[(4-methoxy benzoyl) oxy] methyl benzoic acid}) L1 , and (2-{[4-methyl benzoyl] oxy methyl } benzoic acid) L2 and the interaction of these binary complexes with nucleotides (5′-AMP , 5′-GMP , 5′-IMP , 5′-CMP , 5′-ADP , and 5′-ATP) and CT–DNA for possible CT-*DNA* quantification. The present study can be considered as a continuation for the author work in the field of analytical applications of lanthanide complexes [42–51].

Experimental

Chemicals

All materials employed in the present investigation were of A.R grade products. Guanosine 5′-monophosphate (5′-GMP), inosine 5′-monophosphate (5′-IMP), adenosine 5′-monophosphate (5′-AMP), cytidine 5′-monophosphate (5′-CMP) were purchased from Sigma chemical Co. and were used without purification. Reagent-grade phloroglucinol (PG) 1, 3, 5-trihydroxybenzene ,(2-{[(4-methoxy benzoyl) oxy] methyl benzoic acid}) (L1), (2-{[4-methyl benzoyl] oxy methyl } benzoic acid) (L2) were purchased from Sigma Chemical Co,ST.Louis, Mo. p-toulene sulfonate (PTS) was from Merck AG, Darmstadt, Germany. $EuCl_3.6H_2O$, was from sigma chemical Co .Stock solutions of metal salt were prepared by dissolving precisely weighed amounts of the salt in bidistilled water. Calf thymus DNA (CT–DNA) was obtained from Sigma-Aldrich Biotech. Co., Ltd.

Deionized double-distilled water and analytical grade reagents were used throughout. CT–DNA stock solution was prepared by dissolving the solid material in 5 mM phosphate buffer (pH 7.00) containing 50 mM NaCl. The CT–DNA concentration in terms of base pair L^{-1} was determined spectrophotometrically by employing an extinction coefficient of 13,200 M^{-1} cm^{-1} (base pair) $^{-1}$ at 260 nm. The CT–DNA concentration in terms of nucleotide l^{-1} was also determined spectrophotometrically by employing an extinction coefficient of 6,600 M^{-1} cm^{-1} (nucleotide) $^{-1}$ at 260 nm.

These CT–DNA solutions were stored at 4 °C for more than 24 h with gentle shaking occasionally to get homogeneity and used within 5 days.

The structures of the ligands under investigation are given in Scheme 1.

Apparatus

Cyclic voltammetry (CV), square wave voltammetry (SWV), differential pulse voltammetry (DPP) were collected using EG&G Princeton Applied Research, potentiostat / galvanostat model 263 with a single compartment voltammetric cell equipped with a glassy carbon (GC) working electrode (area=0.1963 cm^3) embedded in a resin .The glassy carbon electrode was polished with γ-Al_2O_3 suspension of 0.1 μm particle size on polishing cloth (Mark V Laboratory, East Granby,CT).

A Pt-wire counter electrode, and saturated calomel electrode as reference electrode were used. A perkin Elmer UV-visible automatic recording spectrophotometer with 1 cm quartz cell was used for the absorbance and spectral UV-visible measurements. Elemental analyses of C, N and H were carried out on an Elemental Vario EL analyzer. The metal ion content was determined by complexo-metric titration with EDTA after destruction of the complex in the conventional manner. The IR spectra were recorded on a Nicolet Nexus 670 FT-IR spectrometer using KBr disc in the 4000–400 cm^{-1} region. The fluorecence of the binary and ternary complexes were scanned on A JASCO-FP6300 spectrofluorometer using 1 cm quartz cell for the emission and spectral measurements.

Scheme 1 Structures of the ligands under investigation

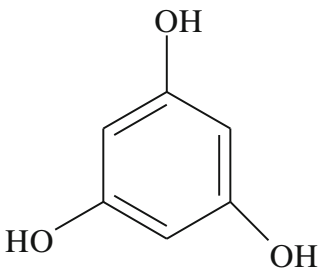

Phloroglucinol (PG) (1, 3, 5-trihydroxybenzene)

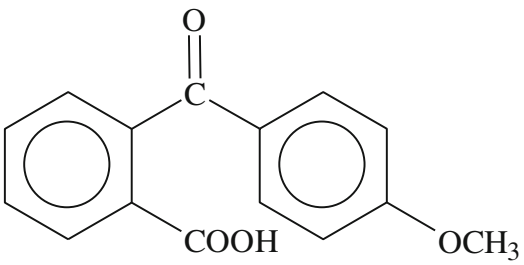

(2-{[(4-methoxy benzoyl) oxy] methyl benzoic acid }) L1

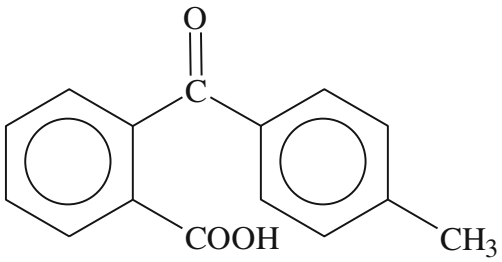

(2-{[4-methyl benzoyl] oxy methyl } benzoic acid) L2

Procedure for Electrochemical Measurements

A typical experiment had a sample volume of 10 cm3 containing:

(a) 5.10^{-4}mol dm^{-3} Eu(III)
(b) 5.10^{-4}mol dm^{-3} Eu(III)+5.10^{-4}mol dm^{-3} nucleotide
(c) 5.10^{-4}mol dm^{-3} Eu(III)+5.10^{-4}mol dm^{-3}L1 or L2
(d) 5.10^{-4}mol dm^{-3} Eu(III)+5.10^{-4}mol dm^{-3} nucleotide+ 5.10^{-4}mol dm^{-3}L1 or L2.

The ionic strength of the studied solutions was adjusted at 0.1 using 0.1 M p-toluene sulfonate solution.

For cyclic voltammetry, the solution was purged with nitrogen for 60–120 second (s) and then the potential was scanned at scan rate 100mVs^{-1}.

For square wave voltammery , the sample were analyzed also as in cyclic voltammetry, the pulse height was 25 mV, frequency was 80 Hz and the scan increment was 2.0 mV.

For differential pulse voltammetry, the samples were analyzed also as in cyclic voltammetry, but at a scan rate= 36.6 mVs^{-1}. The pulse height was 25 mV, the pulse width= 5.10^{-1}s, frequency was 20 Hz and the scan increment was 2.0 mV.

Procedure for Spectrophotometric Measurements

UV and Visible Spectra

The measurements were conducted according to the following scheme:

(1) 5.10^{-4}mol dm^{-3} Eu(III)
(2) 5.10^{-4}mol dm^{-3} Eu(III)+5.10^{-4}mol dm^{-3} ligand (L, L1, and L2) where

L=Phloroglucinol ligand (1, 3, 5 trihydroxy benzene (PG)
L1=(2-{[(4-methoxy benzoyl) oxy] methyl benzoic acid}) L2=(2-{[4-methyl benzoyl] oxy methyl }benzoic acid).

The UV absorption spectra of the solid ligands in ethanol solution were scanned from 200–400 nm against ethanol as a blank .For the binary metal ion complexes 50 % v/v ethanol-water mixture solution was used. For ternary metal ion complexes the same procedure was operated.After

UV absorption spectra fluorescence measurerments for the above metal ion complex solutions have been carried out.

Synthesis of Solid Complexes Preparation of (2-{[(4-methoxy benzoyl) oxy] methyl benzoic acid}) L1**:**A solution of 13.34 g (10 mmol) of powdered anhydrous aluminum chloride in 30 ml of nitrobenzene was added dropwise over a period of 40 min to a solution of 4.4 ml (40 mmol) of anisole and 7.4 g (50 mmol) of phthalic anhydride in 120 ml of nitrobenzene while stirring at room temperature. The mixture was stirred for 5.5 h at room temperature, poured into a mixture of 600 ml of 20% hydrochloric acid and 400 g of ice, and treated with ether . The combined extracts were washed with water and with a saturated solution of $NaHCO_3$. The alkaline extract was washed with diethyl ether and acidified with 10% hydrochloric acid. The colorless precipitate was filtered off and dried. Yield 10.8 g (85%), mp 130–132 °C.

Preparation of (2-{[4-methyl benzoyl] oxymethyl } benzoic acid) L2**:** Aluminum chloride is very hygroscopic and releases hydrogen chloride upon reaction with water, including moisture in the air. It should be stored in a dessicator jar. The aluminum chloride should be weighed in a small, dry, stoppered vial or reaction tube on the balance in the hood at desk number 3. The quality of the aluminum chloride determines the success of the experiment. Into a dry 10×100 mm reaction tube 150 mg of phthalic anhydride was placed and 0.75 mL of anhydrous toluene was added. The mixture was cooled in an ice bath, and then 300 mg of anhydrous aluminum chloride was added. (Note: Aluminum chloride is very moisture sensitive and should be weighed quickly. Cap the bottle immediately after use). Cap the tube with a septum connected to Teflon tubing leading to another reaction tube, which contains a piece of damp cotton to act as a trap for the hydrogen chloride liberated in the reaction. To thread a Teflon tube through a septum, make a hole through the septum with a needle, and then push a toothpick through the hole. Push the Teflon tube firmly onto the toothpick, and then pull and push on the toothpick. The tube will slide through the septum. Finally, pull the tube from the toothpick. Mix the contents of the tube thoroughly by flicking the tube. Warm the tube by the heat of the hand. If the reaction does not start, warm the tube very gently in a beaker of warm water or hold it over the sand bath for a few seconds. At the first sign of vigorous boiling or evolution of hydrogen chloride (as evidenced by testing the gas coming out of the end of the teflon tube on a wet piece of pH test paper), hold the tube over the ice bath in readiness to cool it if the reaction becomes too vigorous. Continue this gentle, cautious heating until the reaction proceeds smoothly enough to reflux it on the hot sand bath. This will take about 5 min. Heat the reaction mixture on the sand bath until evolution of hydrogen chloride almost ceases, then cool it in ice, and add around 1 g of ice in small pieces. Allow each little piece to react before adding the next. Mix the reaction mixture well during this hydrolysis using a glass rod. After the reaction subsides, add 0.1 mL of concentrated hydrochloric acid and 1 mL of water. Mix the contents of the tube thoroughly, and make sure the mixture is at room temperature. Add 0.5 mL more water, mix the solution

well, ascertain that it is at room temperature, and then add 1.5 mL of ether (use the wet ether found in a supply bottle in each hood) and break up any lumps in the tube with a stirring rod. Stopper the tube and shake it vigorously to complete the hydrolysis and extraction. Allow the layers to separate, and then remove the aqueous layer with a Pasteur pipette. Add 0.1 mL of concentrated hydrochloric acid and 0.15 mL of water. Shake the mixture vigorously again, and remove the aqueous layers. Transfer the organic layers to a small test tube containing calcium chloride pellets. Allow the solution to dry for 5 min, and then transfer it back to the clean dry reaction tube, rinsing the drying agent with a small quantity of ether. Add a boiling chip, and boil off the solvents until the volume in the tube is 0.5 mL, then add hexanes until the solution is slightly turbid, indicating that the product is beginning to crystallize. Allow the product to crystallize at room temperature and then at 0 °C. Collect the crystals on the Hirsch. Pure 2-(4-methylbenzoyl)benzoic acid melts at 138 to 139 °C, the yield should be about 0.2 g.

Procedure for Fluorescence Determination of CT–DNA

The fluorescence spectra and intensities were monitored at the fixed analytical emission wavelength (λ_{em}=613 nm) of the complex in aqueous solution. Fluorescence titrations were performed in a 1 cm quartz cuvette by successive addition of DNA ($1–35\times10^{-6}$ M) to solutions of 1.0×10^{-5} M Eu(III)-L2 complex. Before reacting Eu(III) complex with CT–DNA, its solution behavior in the phosphate buffer solution pH 7.0 at room temperature was monitored by UV–vis and fluorescence measurments for 24 h. Liberation of the ligand was not observed under these conditions. These suggest that the complexes are stable under the conditions studied. Under optimal conditions in phosphate buffer pH 7.0 at 25 °C the linear range is 3–20 μM for calf thymus DNA (CT- DNA) and the corresponding determination limit is1.8 μM.

Preparation of Eu(III)-complexes

To a solution containing (3 mmol) $EuCL_3.6H_2O$ (2-{[(4-methoxy benzoyl) oxy] methyl benzoic acid}) L1 or (2-{[4-methyl benzoyl] oxy methyl} benzoic acid) (6 mmol) L2 was added in 30 cm^3 distilled water . After stirring for about 30 min, the pH value was adjusted to 4.00 by adding NaOH .

The mixture was stirred and heated or refluxed on heater for (3 h),then the products were cooled and crystallize out, the complexes were collected by washing with ethanol or diethyl ether. Finally, the complexes were dried in vacuo.

Viscosity Titration Experiments

Viscosity measurements for different CT–DNA solutions containing Eu(III)-L1 or L2 complexes were carried on an Ubbelohde viscometer in a thermostated water bath maintained at (25.0±0.1) °C . Titrations were performed for an investigated compound that was introduced into CT–DNA solution (50 mM, bps) present in the viscometer. Relative viscosities for DNA in either the presence or absence of compound were calculated [52].

Prepration of DNA Solution

Calf thymus DNA (CT–DNA) was obtained from Sigma-Aldrich Biotech. Co., Ltd. Deionized double-distilled water and analytical grade reagents were used throughout. CT–DNA stock solution was prepared by dissolving the solid material in 5 mM phosphate buffer (pH 7.00) containing 50 mM NaCl. The CT–DNA concentration in terms of base pair L^{-1} was determined spectrophotometrically by employing an extinction coefficient of 13,200 M^{-1} cm^{-1} (base pair) $^{-1}$ at 260 nm. The CT–DNA concentration in terms of nucleotide l^{-1} was also determined spectrophotometrically by employing an extinction coefficient of 6,600 M^{-1} cm^{-1} (nucleotide) $^{-1}$ at 260 nm.

These CT–DNA solutions were stored at 4 °C for more than 24 h with gentle shaking occasionally to get homogeneity and used within 5 days.

Results and Dissection

Electrochemical studies of the ternary systems of the type Eu(III) -L1 or L2-nucleotide Representative cyclic voltammograms for Eu(III) –nucleotide-L1 or L2 systems are shown in Figs. 1, 2, 3 and 4. It is clearly observed that the reduction process of Eu(III) metal ions proceeds via quasi – reversible electro chemical process at the glassy carbon electrodes involving one electron transfer step based on the electrichemical analysis of the given cyclovotammograms .

The voltammetric data for the systems under investigations are collected in Tables 1, 2, 3, 4 and 5. Inspecting the obtained voltammograms one can observe that the binding of 5′-GMP molecule with the aquo complex of Eu(III) will shift the reduction potential to less negative value by about 21 mV . The reaction of Eu(III) with L1 will shift the reduction potential slightly , while L2 shifts the potential to more positive value by 96 mV i.e. the binding of L2 to Eu (III) will facilitate the reduction of the corresponding binary species .

For the anodic reaction, the binding of 5′-GMP to Eu(III) will increase the oxidation potential to more positive value . Also the two binary complexes of L1 and L2 are oxidized

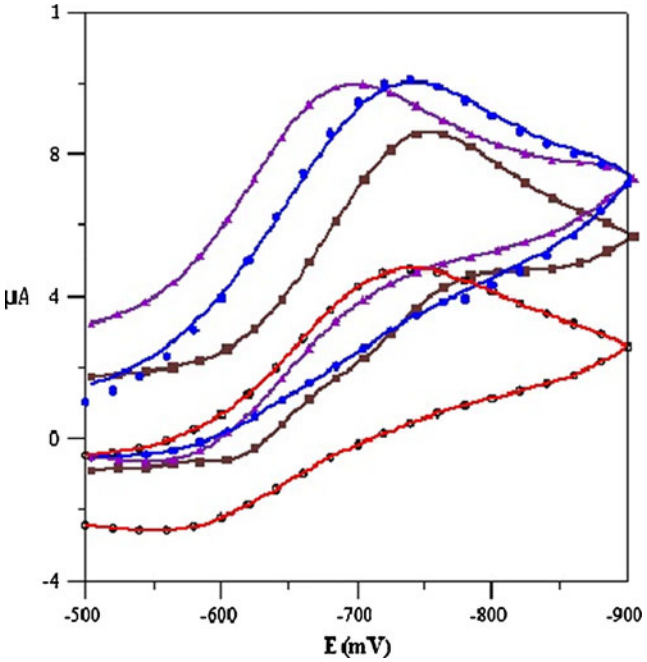

Fig. 1 Cyclic voltammograms for Eu(III)-5′-AMP-(2-{[(4-methoxy benzoyl) oxy]methyl benzoic acid}) system in 0.1 mol dm^{-3} p-toluene sulfonate , scan rate=100 mV s^{-1} and at 25°C. ○ 5×10^{-4} mol dm^{-3} Eu (III) ——. ● 5×10^{-4} mol dm^{-3} Eu(III)+5×10^{-4} mol dm^{-3} 5′-AMP 1:1 ——. ■ 5×10^{-4} mol dm^{-3} Eu(III)+5×10^{-4} mol dm^{-3} (2-{[(4-methoxy benzoyl) oxy]methyl benzoic acid}) ——. ▲ 5×10^{-4} mol dm^{-3} Eu(III)+5×10^{-4} mol dm^{-3} 5′-AMP+5×10^{-4} mol dm^{-3} (2-{[(4-methoxy benzoyl) oxy]methyl benzoic acid}) ——

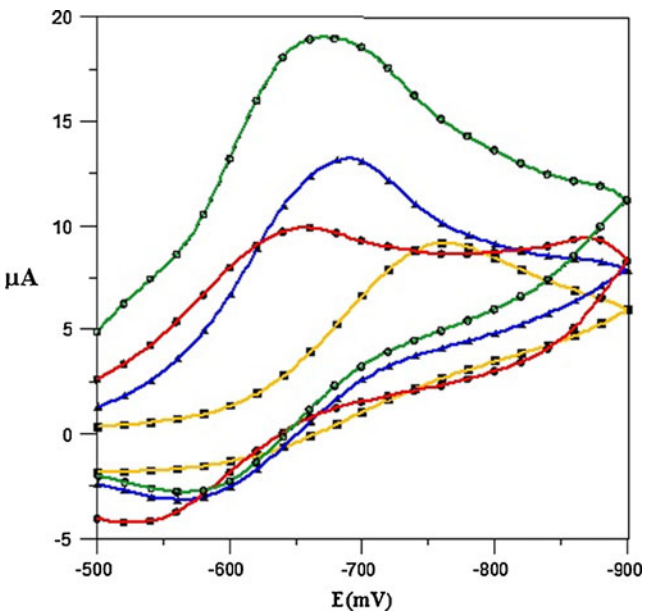

Fig. 2 Cyclic voltammograms for Eu(III) -5′-IMP- (2-{[(4-methoxy benzoyl) oxy]methyl benzoic acid}) system in 0.1 mol dm^{-3} p-toluene sulfonate , scan rate=100 mV s^{-1} and at 25°C. ● 5×10^{-4} mol dm^{-3} Eu (III) ——. ○ 5×10^{-4} mol dm^{-3} Eu(III)+5×10^{-4} mol dm^{-3} 5′-IMP 1:1 ——. ■ 5×10^{-4} mol dm^{-3} Eu(III)+5×10^{-4} mol dm^{-3} (2-{[(4-methoxy benzoyl) oxy]methyl benzoic acid}) ——. ▲ 5×10^{-4} mol dm^{-3} Eu(III)+5×10^{-4} mol dm^{-3} 5′-IMP+5×10-4 mol dm^{-3}. (2-{[(4-methoxy benzoyl) oxy]methyl benzoic acid}) ——

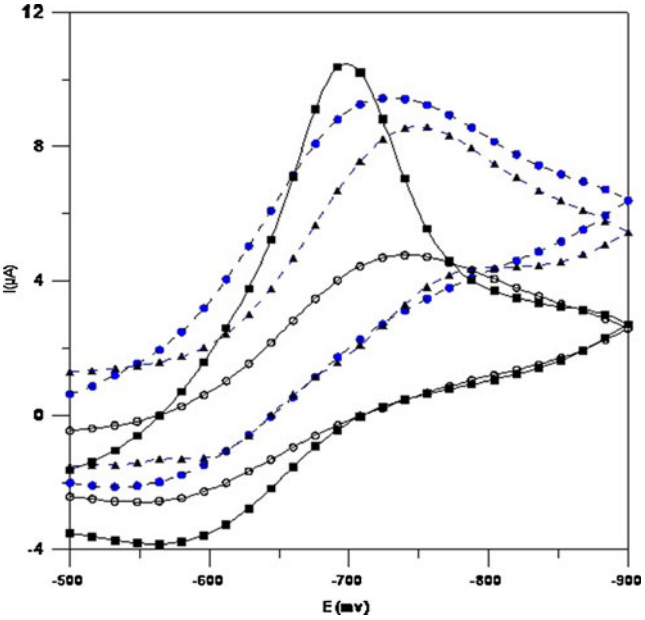

Fig. 3 Cyclic voltammograms for Eu(III) -5′-GMP-(2-{[(4-methoxy benzoyl) oxy]methyl benzoic acid}) system in 0.1 mol dm^{-3} p-toluene sulfonate , scan rate=100 mV s^{-1} and at 25 °C. ○ 5×10^{-4} mol dm^{-3} Eu (III) ——. ● 5×10^{-4} mol dm^{-3} Eu(III)+5×10^{-4} mol dm^{-3} 5′-GMP 1:1 – – – – –. ▲ 5×10^{-4} mol dm^{-3} Eu(III)+5×10^{-4} mol dm^{-3} (2-{[(4-methoxy benzoyl) oxy]methyl benzoic acid}) – – – – –. ■ 5×10^{-4} mol dm^{-3} Eu(III)+5×10^{-4} mol dm^{-3} 5′-GMP+5×10^{-4} mol dm^{-3} (2-{[(4-methoxy benzoyl) oxy]methyl benzoic acid}) ——

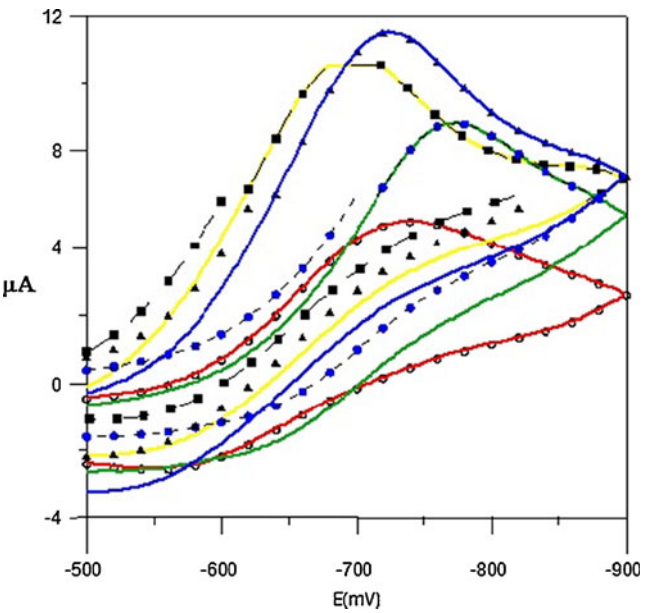

Fig. 4 Cyclic voltammograms for Eu(III)-5′-ATP- (2-{[4-methyl benzoyl] oxy methyl }benzoic acid) system in 0.1 mol dm^{-3} P-toluene sulfonate , scan rate=100 mV s^{-1} and at 25 °C. ○ $5\times10^{-4}5\times$ 10-4 mol dm^{-3} Eu(III) ——. ■ 5×10^{-4} mol dm^{-3} Eu(III)+$5\times$ 10^{-4} mol dm^{-3} 5′-ATP 1:1 ——. ● 5×10^{-4} mol dm^{-3} Eu(III)+ 5×10^{-4} mol dm^{-3} (2-{[4-methyl benzoyl] oxy methyl }benzoic acid) – – – – –. ▲ 5×10^{-4} mol dm^{-3} Eu(III)+5×10^{-4} mol dm^{-3} 5′-ATP+ 5×10^{-4} mol dm^{-3} (2-{[4-methyl benzoyl] oxy methyl }benzoic acid) ——

Table 1 Voltammetric data for Eu(III)-5′- AMP -L1 or L2 dm^{-3} in 0.1 mol p-toluene sulfonic acid at 25 °C

System	-Ep,c (mV)	-Ep,a (mV)	(Ep,c-Ep,a)	Ip,c (μA)	Ip,a (μA)	α	$(D)_{red}$(cm s^{-1})	$(D)_{ox}$ (cm s^{-1})	K (cm s^{-1})
Eu(III)	750.26	545.2	205.06	4.83	2.37	0.296	3.354×10^{-13}	8.12×10^{-14}	3.88×10^{-12}
Eu(III)+AMP	740.7	549.6	189.1	10.22	1.26	0.339	1.501×10^{-12}	2.29×10^{-14}	3.38×10^{-12}
Eu(III)+L1	750.8	565.7	185.1	8.56	1.72	0.377	1.053×10^{-12}	4.25×10^{-14}	2.72×10^{-12}
Eu(III)+L2	786.7	570.4	216.3	9.23	1.84	0.2855	1.225×10^{-12}	4.87×10^{-14}	3.15×10^{-12}
Eu(III)+AMP+L1	711.6	561.3	150.3	10.14	1.93	0.348	1.479×10^{-12}	5.36×10^{-14}	1.86×10^{-12}
Eu(III)+AMP+L2	763.4	555.2	108.2	8.52	1.91	0.2461	1.043×10^{-12}	5.24×10^{-14}	1.54×10^{-12}

L1=(2-{[(4-methoxy benzoyl) oxy] methyl benzoic acid}) L2=(2-{[4-methyl benzoyl] oxy methyl } benzoic acid)

at higher oxidation potentials than the free metal ion. The ternary complex species involving Eu(III) 5′-GMP with the two ligands (L1 and L2) resist the oxidation through the increase in oxidation potential of the two complexes especially in the case of L1 .

Upon reacting of L2 with Eu(III)- 5′-AMP, the reduction potential of ternary complexes is shifted to less negative value in contrary to L 2 where the mixed ligand complex is reduced at more negative potential i.e. the latter will be reduced more hardly .For the two ternary complex species ,they are oxidized at more positive potential in somewhat a little manner than the binary complex Eu(III) 5′-AMP. It is clearly observed that the binding of Eu(III)- 5′-AMP to free Eu(III) will cause a very little shift in reduction potential .

The binding of Eu(III)- 5′-IMP molecule with Eu(III) will shift the reduction potential to less negative value i.e., Eu(III)- 5′-IMP is easily reduced than the free metal Eu(III) . Upon reacting of either L1or L2 with Eu(III)- 5′-IMP the reduction potential was shifted to more negative value where this shift was considerable in the case of L1. For the oxidation process the ternary complexes are oxidized at more positive potentials in somewhat the same manner for the two ligands L1 and L2 .

After the addition of L1 to a solution containing Eu(III)-5′-ADP binary complex the reduction potential was shifted to more negative value while the reaction of L2 with Eu (III)- 5′-ADP will shift the reduction potential to less negative value .The interaction of either L1 or L2 with Eu (III)- 5′-ADP will shift the oxidation potential to more positive by about 12.0 and 23.0 mV, respectively . The binary complex of Eu(III) -5′-ADP is easily reduced than the free metal ion .

The corresponding ternary complexes species of the type Eu(III)- 5′-ATP -L1 or L2 are hardly reduced than the binary 5′-ATP as indicated by the shift in the reduction potential to more negative value especially in the case of L1. .A slight positive shift is observed for 5′-ATP upon binding to either L1 or L2 . The nucleotide molecule 5′-ATP upon reacting with Eu(III) will shift the reduction potential to less negative in a considerable value , while the oxidation potential is slightly shifted to less positive value.

Generally upon reaction of the nucleotide molecules with Eu(III) the reduction potential of the complexes are decreased according to the following order : 5′-IMP >5′-ATP>5′-ADP >5′-GMP >5′-AMP . On the other hand, for the oxidation process, the oxidation potential of the binary complexes is increased in the following sequence: 5′-IMP> 5′-ADP>5′-GMP>5′-AMP, while for 5′-ATP the oxidation potential is decreased. For the ternary complexes Eu(III)-Nucleotide-L1 the sequence of the reduction potential with respective to the nature of the nucleotide molecule is :

5′-ATP>5′-ADP>5′-AMP >5′-GMP≈5′-IMP while for those containing L2 the order is 5′-AMP>5′-ATP>5′-GMP>

Table 2 Voltammetric data for Eu(III)-5′-GMP -L1 or L2 in 0.1 mol dm^{-3} p-toluene sulfonic acid at 25 °C

System	-Ep,c (mV)	-Ep,a (mV)	(Ep,c-Ep,a)	Ip,c (μA)	Ip,a (μA)	α	$(D)_{red}$(cm s^{-1})	$(D)_{ox}$(cm s^{-1})	K (cm s^{-1})
Eu(III)	750.26	545.2	205.06	4.83	2.37	0.296	3.35×10^{-13}	8.12×10^{-13}	3.88×10^{-12}
Eu(III)+GMP	728.6	558.4	170.2	9.85	1.26	0.370	1.395×10^{-12}	4.82×10^{-14}	2.88×10^{-12}
Eu(III)+L1	750.8	565.7	185.1	8.56	1.72	0.377	1.05×10^{-12}	4.25×10^{-14}	2.72×10^{-12}
Eu(III)+L2	786.7	570.4	216.3	9.23	1.84	0.285	1.225×10^{-12}	4.87×10^{-14}	3.15×10^{-12}
Eu(III)+GMP+L1	702.7	582.3	120.4	11.35	1.93	0.463	1.361×10^{-12}	1.97×10^{-13}	7.01×10^{-12}
Eu(III)+GMP+L2	710.4	570.7	139.7	9.31	0.63	0.395	1.246×10^{-12}	5.70×10^{-15}	4.36×10^{-12}

L1=(2-{[(4-methoxy benzoyl) oxy] methyl benzoic acid}) L2=(2-{[4-methyl benzoyl] oxy methyl } benzoic acid)

Table 3 Voltammetric data for Eu(III)-5′-IMP -L1 or L2 in 0.1 mol dm^{-3} p-toluene sulfonic acid at 25 °C

System	-Ep,c (mV)	-Ep,a (mV)	(Ep,c-Ep,a)	Ip,c (μA)	Ip,a (μA)	α	$(D)_{red}$(cm s^{-1})	$(D)_{ox}$ (cm s^{-1})	K (cm s^{-1})
Eu(III)	750.26	545.2	205.06	4.83	2.37	0.296	3.354×10^{-13}	8.10×10^{-14}	3.88×10^{-12}
Eu(III)+IMP	665.4	560.1	105.3	18.62	2.74	0.4515	4.985×10^{-12}	1.07×10^{-13}	5.06×10^{-12}
Eu(III)+L1	750.8	565.7	185.1	8.56	1.72	0.377	1.053×10^{-12}	4.25×10^{-14}	2.72×10^{-12}
Eu(III)+L2	786.7	570.7	139.7	9.31	0.63	0.2855	1.225×10^{-12}	4.87×10^{-14}	3.15×10^{-12}
Eu(III)+IMP+L1	702.7	582.3	120.4	11.35	1.93	0.463	1.723×10^{-12}	1.44×10^{-14}	9.93×10^{-12}
Eu(III)+IMP+L2	674.2	585.4	89.8	10.28	2.72	0.416	1.519×10^{-12}	1.06×10^{-13}	3.80×10^{-12}

L1=(2-{[(4-methoxy benzoyl) oxy] methyl benzoic acid}) L2=(2-{[4-methyl benzoyl] oxy methyl } benzoic acid)

5′-IMP≈5′-ADP. According to the nature of nucleotides the oxidation reaction of Eu(III)-nucleotide-L1 complexes follow the order: 5′-GMP >5′-IMP>5′-ADP >5′-AMP >5′-ATP while for the ternary complexes containing L2 the order is: 5′-IMP >5′-ADP >5′-GMP>5′-AMP>5′-ATP.

The diffusion coefficients of the reduced and oxidized species are calculated according to the following equations:

$$Ip = 2.69\times10^{5}\times n^{3/2}\times A\times D^{1/2+}\times \upsilon^{1/2}\times Co \qquad (1)$$

where

- Ip current in Ampere.
- N number of electron transfer=1
- D diffusion coefficient in cm^2s^{-1}
- υ scan rate in volt/s=100 mV s^{-1}=0.1 Vs^{-1}
- Co molar concentration of the reactive species=5×10^{-4} A=electrode area=0.196 cm^2
- Ipc cathodic current potential and ipa=anodic current potential
- D_{red} diffusion coefficient of reduced form. D_{ox}=diffusion coefficient of oxidized form.

$$\alpha = 1.857RT/n[Ep - Ep/2]\times F \qquad (2)$$

where (α=transfer coefficient , R=8.31 ,T=298.0 K ,F= 96500). The binary complex species involving Eu(III) with the nucleotide molecules exhibit high values for the diffusion coefficients (D_{red}) in comparison to the free metal ion Eu(III). The order of increase for the diffusion coefficients is as follows : 5′-IMP >5′-ATP >5′-AMP>5′-GMP>5′-ADP. The free metal ion Eu(III) exhibits nearly reversible process since the diffusion coefficients of the reduced or oxidized species are normally the same. Upon reduction of Eu(III)-nucleotide complexes i.e. the complex species containing Eu(III) the diffusion coefficients are generally increased with regard to to the free metal ion .The order of increasing for the nucleotides is: 5′-IMP >5′-ATP> 5′-AMP>5′-GMP >5′-ADP.

The complex of Eu(III) with L1 and L2 have higher diffusion coefficients than the free metal ion , the increase in the case of methyl derivative is higher than in the case of methoxy one. It is clearly observed that the reaction of either L1 or L2 with the binary complex Eu(III)- 5′-GMP forming the corresponding ternary complex is accompanied by a slight decrease in the diffusion coefficients of ternary species . The interaction of L1 with Eu(III)- 5′-AMP binary complex has no significant effect on the diffusion coefficient of the produced mixed ligand complex, while in the case of L2 the species Eu(III)- 5′-AMP-L2 has lower value than the corresponding Eu(III)- 5′-AMP complex .A considerable dramatic decrease in the diffusion coefficient of the ternary species Eu(III)- 5′-IMP upon reacting with either L1 or L2 has been observed. L1 doesn't exhibit significant change in the diffusion coefficient for Eu(III)-5′-ADP upon reacting with this species forming the ternary one .On the other hand the ternary complex Eu(III)- 5′-ADP-L2 has a higher diffusion coefficient value than the binary metal ion –nucleotide species . A large increase in the value of

Table 4 Voltammetric data for Eu(III)-5′-ADP -L1 or L2 in 0.1 mol dm^{-3} p-toluene sulfonic acid at 25 °C

System	-Ep,c (mV)	-Ep,a (mV)	(Ep,c-Ep,a)	Ip,c (μA)	Ip,a (μA)	α	$(D)_{red}$(cm s^{-1})	$(D)_{ox}$ (cm s^{-1})	K (cm s^{-1})
Eu(III)	750.26	545.2	205.06	4.83	2.37	0.2991	3.354×10^{-13}	8.10×10^{-14}	3.88×10^{-12}
Eu(III)+ADP	709.1	559.3	149.8	8.61	1.95	0.4515	1.066×10^{-12}	5.46×10^{-12}	1.07×10^{-12}
Eu(III)+L1	750.8	565.7	185.1	8.56	1.72	0.3783	1.053×10^{-12}	4.25×10^{-14}	2.72×10^{-12}
Eu(III)+L2	786.7	570.7	139.7	9.31	0.63	0.2855	1.225×10^{-12}	4.87×10^{-14}	3.15×10^{-12}
Eu(III)+ADP+L1	761.2	571.4	189.8	8.36	1.54	0.2953	1.004×10^{-12}	3.41×10^{-14}	2.014×10^{-12}
Eu(III)+ADP+L2	672.7	582.4	90.3	11.34	2.11	0.4419	1.848×10^{-12}	6.41×10^{-14}	2.29×10^{-12}

L1=(2-{[(4-methoxy benzoyl) oxy] methyl benzoic acid}) L2=(2-{[4-methyl benzoyl] oxy methyl } benzoic acid)

Table 5 Voltammetric data for Eu(III)-5′-ATP -L1 or L2 in 0.1 mol dm^{-3} p-toluene sulfonic acid at 25 °C

System	-Ep,c (mV)	-Ep,a (mV)	(Ep,c-Ep,a)	Ip,c (μA)	Ip,a (μA)	α	$(D)_{red}$ cm s^{-1}	$(D)_{ox}$ (cm s^{-1})	K (cm s^{-1})
Eu(III)	750.26	545.2	205.06	4.83	2.37	0.2991	3.354×10^{-13}	8.10×10^{-14}	3.88×10^{-12}
Eu(III)+ATP	701.7	531.3	170.4	11.13	1.64	0.4463	1.781×10^{-12}	3.87×10^{-14}	2.93×10^{-12}
Eu(III)+L1	750.8	565.7	185.1	8.56	1.72	0.3783	1.053×10^{-12}	4.25×10^{-14}	2.72×10^{-12}
Eu(III)+L2	768.7	570.7	139.7	9.31	0.63	0.2855	1.225×10^{-12}	4.87×10^{-14}	3.15×10^{-12}
Eu(III)+ATP+L1	769.1	559.8	209.3	8.14	1.90	0.3862	9.534×10^{-12}	5.19×10^{-14}	1.48×10^{-12}
Eu(III)+ATP+L2	739.3	534.6	204.7	11.65	2.09	0.3681	1.951×10^{-12}	6.28×10^{-14}	4.58×10^{-12}

L1=(2-{[(4-methoxy benzoyl) oxy] methyl benzoic acid}) L2=(2-{[4-methyl benzoyl] oxy methyl } benzoic acid)

the diffusion coefficient of the ternary species Eu(III)- 5′-ATP-L1 in comparison to the binary Eu(III)- 5′-ATP was detected. A slight increase in the diffusion coefficient of the ternary species Eu(III)- 5′-ATP-L2 has been given .

L1 and L2 have contradictory effects on the diffusion coefficients of oxidized species with Eu(III)- 5′-GMP, where for L1 the diffusion coefficients value increases while in the case of L2 the diffusion coefficients value decreases.

Upon the reaction of L1 and L2 with Eu(III)–5′-AMP the corresponding ternary complexes acquire higher values for the diffusion coefficients of the oxidized species .

On the other hand, the diffusion coefficients of the ternary complexes are lowered due to the reaction with L1 and L2 . The two nucleotides 5′-ADP and 5′-ATP have different effects on the diffusion coefficients of the oxidized species where the ternary complexes Eu(III)-5′- ADP-L1 or L2 have lower diffusion coefficients than the binary ones while for the species containing 5′-ATP the values are increased .

Figure 5 depicts the effect of variation of scan rate(υ) on the cyclic voltammogram for Eu(III)+5×10^{-4} mol dm^{-3} (2-{[(4-methoxy benzoyl) oxy]methyl benzoic acid}) system. The correlation between cathodic peak current (ip**c**) and square root of scan rate ($\upsilon^{1/2}$) results in a somewhat straight line which indicates that the electro reduction of the different complex species obeys diffusion controlled mechanism .The same behavior was observed for the rest of the ternary systems under investigation .

Confirmation of the formation of binary and ternary complexes of the type Eu(III)-L1 or L2 and Eu(III)-nucleotide-L1 or L2 in solution has been carried out using SWV on a GC electrode. Figures 6, 7, 8, 9, 10, 11, 12, 13, 14 and 15 show the electrochemical square wave voltammograms for representative ternary systems under investigation.

All of the voltammetric diagrams confirm the formation of different binary and ternary complexes that have been found using CV. It is quite interesting to observe that changing the frequency resulted in quite clear changes in the shapes of the square wave voltammograms of the ternary complexes formed in solution, which may be attributed to changing the mechanistic behavior of the electrochemical reduction of the resulting ternary complex on the GC electrode. The reversibility of the electrochemical reaction of binary or ternary complexes in the investigated systems has been studied by CV. The peak separation between the anodic and the cathodic peaks is more than 30 mV. These values indicate that the electrochemical reduction in the case of free Eu(III) ions and Eu (III) binary and ternary complexes under investigation is quasi-reversible on the GC electrode. The electrochemical behaviors of the complexes containing the electroactive metal ion Eu(III) in all of its species are reduced through Eu (III) / Eu(II), that is, a one-electron transfer process.

The more negative shift in the reduction potential of Eu (III)-L2 than Eu(III)-L1 is a good indication of the strong binding of Eu(III) towards L2 .

The stronger shift towards more negative value for Eu (III)- 5′-ADP upon reacting with L2 than L1 indicates the

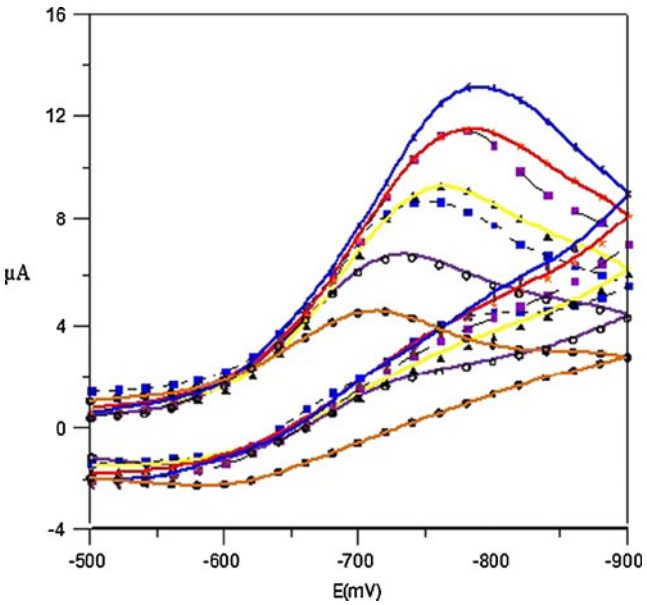

Fig. 5 Effect of scan rate on the cyclic voltammograms for Eu(III)-(2-{[(4-methoxy benzoyl) oxy]methyl benzoic acid}) system in 0.1 mol dm^{-3} p-toluene sulfonate , scan rate=100 mV s^{-1} and at 25 °C. ● Scan rate=50 mV/s ○ Scan rate=75 mV/s ■ Scan rate=100 mV/s ▲ Scan rate=150 mV/s ■ Scan rate=200 mV/s ★ Scan rate=250 mV/s ◖ Scan rate=300 mV/s

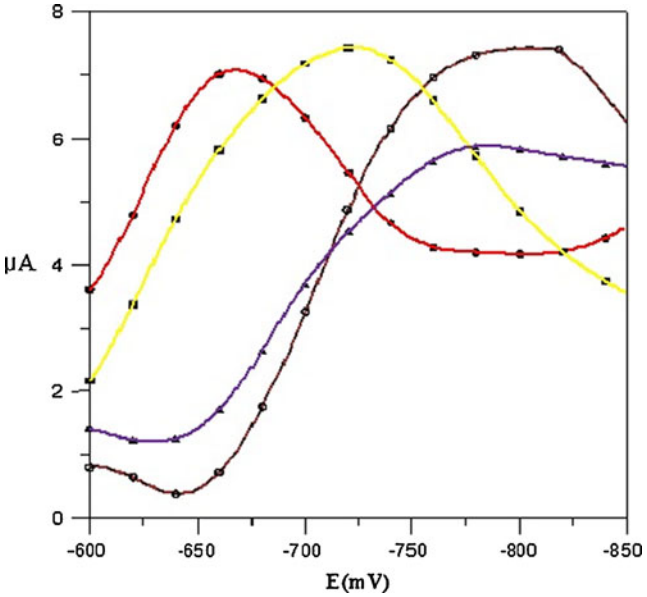

Fig. 6 Square wave voltammogram for Eu(III)-5′-AMP-(2-{[4-methyl benzoyl] oxy methyl }benzoic acid) system in 0.1 mol dm^{-3} p-toluene sulfonate , scan rate=80 mV s^{-1} frequency=60 Hz , and at 25°C. ● 5×10^{-4} mol dm^{-3} Eu(III) ——. ○ 5×10^{-4} mol dm^{-3} Eu (III)+5×10^{-4} mol dm^{-3} 5′-AMP 1:1 ——. ■ 5×10^{-4} mol dm^{-3} Eu(III)+5×10^{-4} mol dm^{-3} (2-{[4-methyl benzoyl] oxy methyl }benzoic acid) ——. ▲ 5×10^{-4} mol dm^{-3} Eu(III)+5×10^{-4} mol dm^{-3} 5′-AMP+5×10^{-4} mol dm^{-3} (2-{[4-methyl benzoyl] oxy methyl }benzoic acid) ——

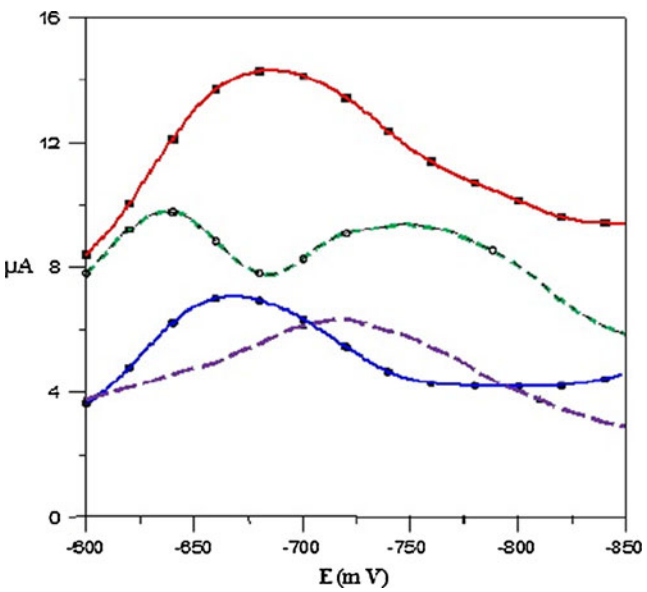

Fig. 7 Square wave voltammograms for Eu(III)-5′-GMP-(2-{[(4-methoxy benzoyl) oxy]methyl benzoic acid}) system in 0.1 mol dm^{-3} p-toluene sulfonate , scan rate=80 mV s^{-1} frequency=60 Hz , and at 25 °C. ● 5×10^{-4} mol dm^{-3} Eu(III) ——. ○ 5×10^{-4} mol dm^{-3} Eu(III)+5×10^{-4} mol dm^{-3} 5′- GMP 1:1 ——. ■ 5×10^{-4} mol dm^{-3} Eu(III)+5×10^{-4} mol dm^{-3} (2-{[(4-methoxy benzoyl) oxy] methyl benzoic acid}) ——. ▲ 5×10^{-4} mol dm^{-3} Eu(III)+5×10^{-4} mol dm^{-3} 5′- GMP+5×10^{-4} mol dm^{-3} (2-{[(4-methoxy benzoyl) oxy] methyl benzoic acid}) ——

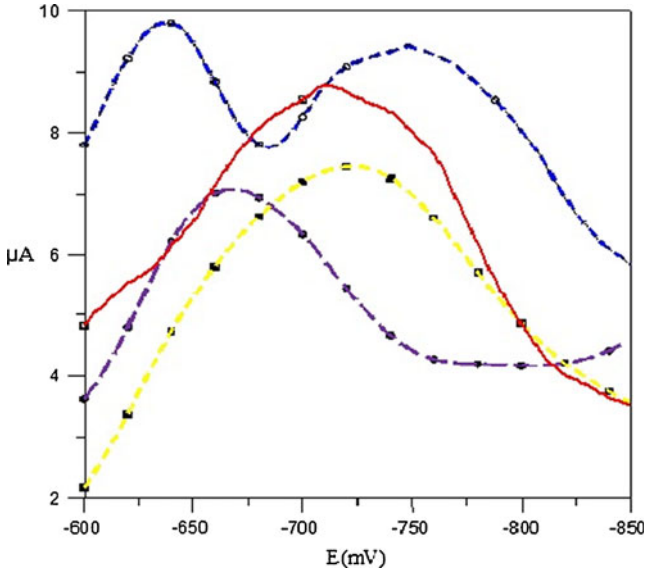

Fig. 8 Square wave voltammograms for Eu(III)-5′-GMP- (2-{[4-methyl benzoyl] oxy methyl }benzoic acid) system in 0.1 mol dm^{-3} p-toluene sulfonate , scan rate=80 mV s^{-1} frequency=60 Hz , and at 25 °C. ● 5×10^{-4} mol dm^{-3} Eu(III) ——. ○ 5×10^{-4} mol dm^{-3} Eu (III)+5×10^{-4} mol dm^{-3} 5′- GMP 1:1 ——. ■ 5×10^{-4} mol dm^{-3} Eu(III)+5×10^{-4} mol dm^{-3} (2-{[4-methyl benzoyl] oxy methyl }benzoic acid) ——. □ 5×10^{-4} mol dm^{-3} Eu(III)+5×10^{-4} mol dm^{-3} 5′-GMP+5×10^{-4} mol dm^{-3} (2-{[4-methyl benzoyl] oxy methyl }benzoic acid) ——

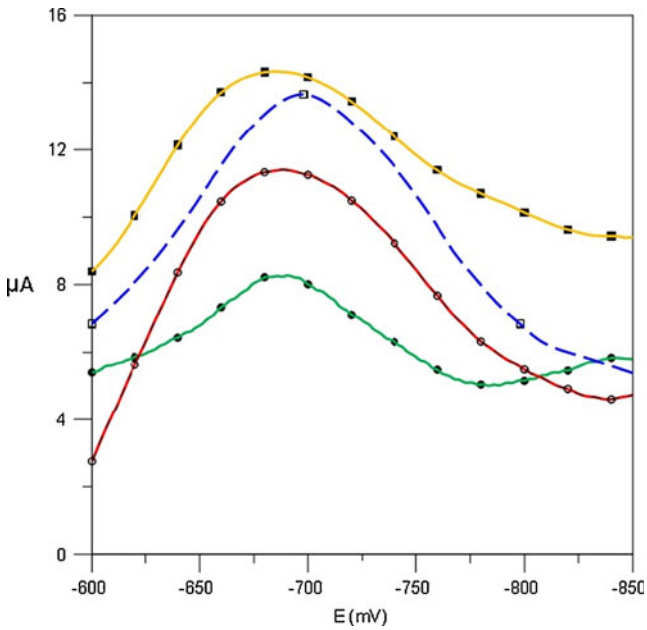

Fig. 9 Square wave voltammograms for Eu(III)-5′-IMP- (2-{[(4-methoxy benzoyl) oxy]methyl benzoic acid}) system in 0.1 mol dm^{-3} p-toluene sulfonate , scan rate=80 mV s^{-1} frequency=60 Hz, and at 25 °C. ● 5×10^{-4} mol dm^{-3} Eu(III) ——. ○ 5×10^{-4} mol dm^{-3} Eu (III)+5×10^{-4} mol dm^{-3} 5′-IMP 1:1 ——. ■ 5×10^{-4} mol dm^{-3} Eu (III)+5×10^{-4} mol dm^{-3} (2-{[(4-methoxy benzoyl) oxy]methyl benzoic acid}) ——. □ 5×10^{-4} mol dm^{-3} Eu(III)+5×10^{-4} mol dm^{-3} 5′-IMP+5×10^{-4} mol dm^{-3} (2-{[(4-methoxy benzoyl) oxy]methyl benzoic acid}) ——

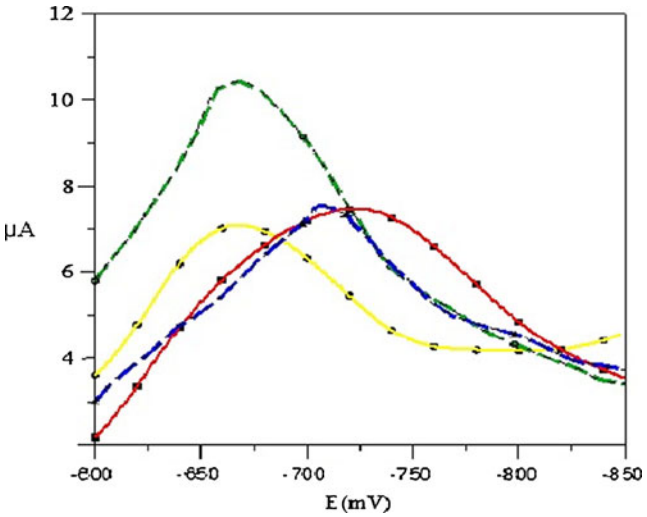

Fig. 10 Square wave voltammograms for Eu(III)-5′-ADP-(2-{[4-methyl benzoyl] oxy methyl }benzoic acid) system in 0.1 mol dm^{-3} p-toluene sulfonate , scan rate=80 mV s^{-1} ,frequency=60 Hz , and at 25 °C. ● 5×10^{-4} mol dm^{-3} Eu(III) ——. ○ 5×10^{-4} mol dm^{-3} Eu(III)+5×10^{-4} mol dm^{-3} 5′-ADP 1:1 – – –. ■ 5×10^{-4} mol dm^{-3} Eu(III)+5×10^{-4} mol dm^{-3} (2-{[4-methyl benzoyl] oxy methyl }benzoic acid) ——. ▲ 5×10^{-4} mol dm^{-3} Eu(III)+5×10^{-4} mol dm^{-3} 5′-ADP+5×10^{-4} mol dm^{-3}(2-{[4-methyl benzoyl] oxy methyl }benzoic acid) – – –

strong binding of L2 towards the binary complex Eu(III)-5′-ADP than L1. Also L2 shows a somewhat binding more probable to Eu(III)- 5′-ATP than L1. The different electro-

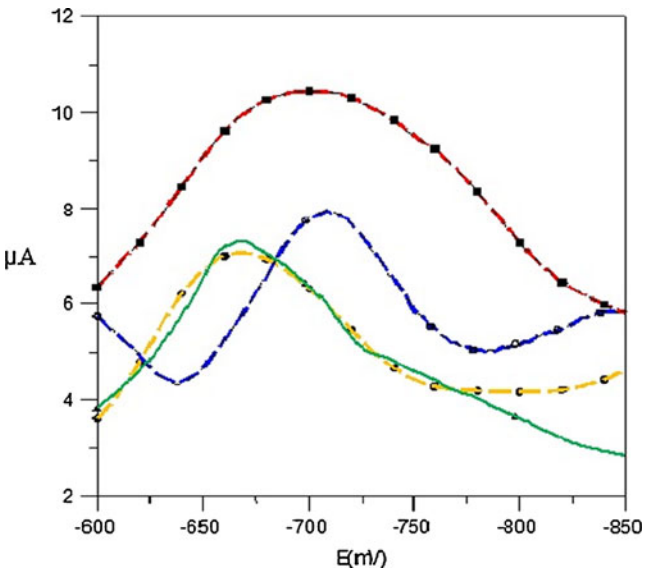

Fig. 11 Square wave voltammograms for Eu(III)-5′-ATP—(2-{[(4-methoxy benzoyl) oxy]methyl benzoic acid}) system in 0.1 mol dm^{-3} p-toluene sulfonate, scan rate=80 mV s^{-1}, frequency=60 Hz, and at 25 °C. ● 5×10^{-4} mol dm^{-3} Eu(III) – – –. ○ 5×10^{-4} mol dm^{-3} Eu(III)+5×10^{-4} mol dm^{-3} 5′-ATP 1:1 – – –. ■ 5×10^{-4} mol dm^{-3} Eu(III)+5×10^{-4} mol dm^{-3} (2-{[(4-methoxy benzoyl) oxy]methyl benzoic acid}) ——. ▲ 5×10^{-4} mol dm^{-3} Eu(III)+5×10^{-4} mol dm^{-3} 5′-ATP+5×10^{-4} mol dm^{-3} (2-{[(4-methoxy benzoyl) oxy]methyl benzoic acid})(2-{[4-methyl benzoyl] oxy methyl }benzoic acid) – – –

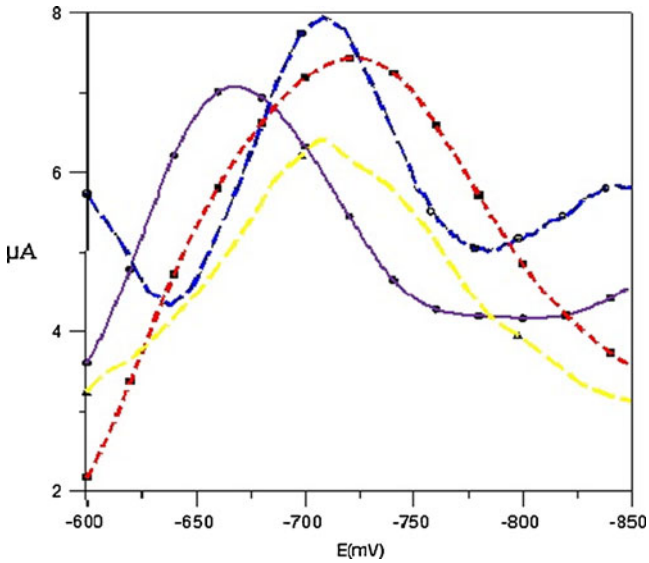

Fig. 12 Square wave voltammograms for Eu(III)-5′-ATP-(2-{[4-methyl benzoyl] oxy methyl }benzoic acid) system in 0.1 mol dm^{-3} p-toluene sulfonate , scan rate=80 mV s^{-1}, frequency=60 Hz, and at 25 °C. ● 5×10^{-4} mol dm^{-3} Eu(III) ——. ○ 5×10^{-4} mol dm^{-3} Eu(III)+5×10^{-4} mol dm^{-3} 5′-ATP 1:1 – – –. ■ 5×10^{-4} mol dm^{-3} Eu(III)+5×10^{-4} mol dm^{-3} (2-{[4-methyl benzoyl] oxy methyl }benzoic acid) – – –. ▲ 5×10^{-4} mol dm^{-3} Eu(III)+5×10^{-4} mol dm^{-3} 5′-ATP+5×10^{-4} mol dm^{-3} (2-{[4-methyl benzoyl] oxy methyl }benzoic acid) – – –

chemical characteristics and some kinetic parameters of the cyclic voltammograms for the systems under investigation are given in Tables 1, 2, 3, 4 and 5.

Kinetic parameters for the above-mentioned binary and ternary Eu(III) complexes have been calculated with the

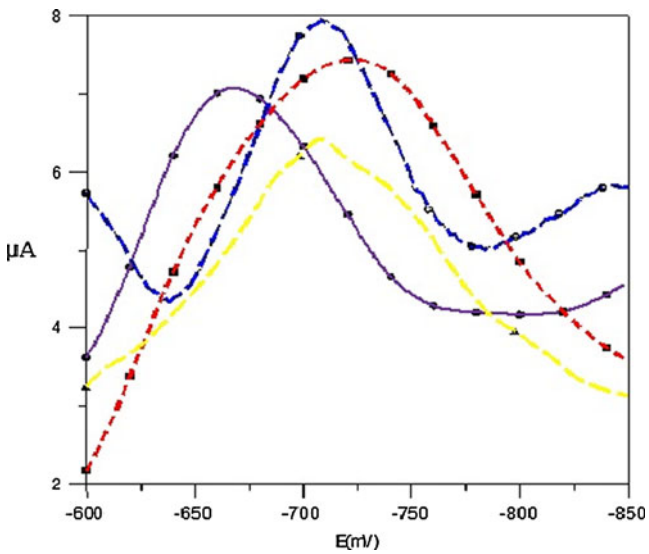

Fig. 13 Effect of frequency on square wave voltammograms for Eu (III)- (2-{[(4-methoxy benzoyl) oxy]methyl benzoic acid}) system in 0.1 mol dm^{-3} p-toluene sulfonate , scan rate=80 mV s^{-1} and at 25 °C. ● Frequency (f=20 Hz) – – – ○ Frequency (f=40 Hz) – – –. ■ Frequency (f=60 Hz) – – – ▲ Frequency (f=80 Hz) – – –

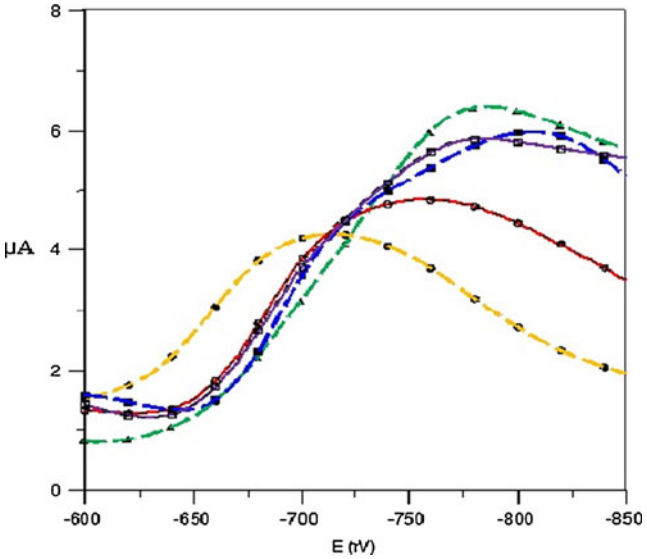

Fig. 14 Effect of frequency on square wave voltammograms for Eu(III)-5′-AMP—(2-{[4-methyl benzoyl] oxy methyl }benzoic acid)system in 0.1 mol dm^{-3} p-toluene sulfonate , scan rate=80 mV s^{-1} and at 25 °C. ● Frequency (f=20 Hz) ▬ ▬ ▬ ○ Frequency (f=40 Hz) ▬▬. ■ Frequency (f=60 Hz) ▬ ▬ ▬ □ Frequency (f= 80 Hz) ▬▬. ▲ Frequency (f=100 Hz) ▬ ▬ ▬

aim to probe their electron transfer ability when used as a basis for biosensors for the electrochemical detection of the nucleotide 5′-AMP , 5′-ADP ,5′-ATP , 5′- GMP , 5′-IMP , and 5′-CMP . So the results obtained in the present work concerning the electrochemical reduction and kinetic parameters calculation for the Eu(III) ternary systems can be considered as a basis for the future development of novel biosensors for the trace determination of these biologically important nucleotides. Even an electrochemluminescence

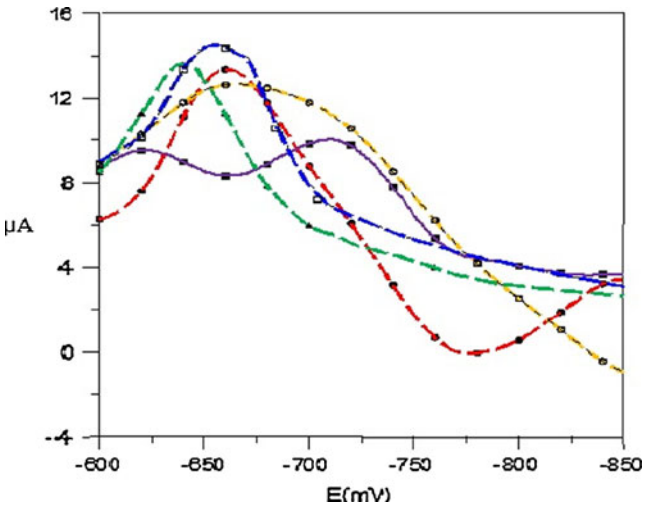

Fig. 15 Effect of frequency on square wave voltammograms for Eu(III)-5′-IMP—(2-{[4-methyl benzoyl] oxy methyl }benzoic acid)system in 0.1 mol dm^{-3} p-toluene sulfonate , scan rate=80 mV s^{-1} and at 25 °C. ● Frequency (f=20 Hz) ▬ ▬ ▬ ○ Frequency (f=40 Hz) ▬ ▬ ▬. ■ Frequency (f=60 Hz) ▬▬ ▲ Frequency (f= 80 Hz) ▬ ▬ ▬. □ Frequency (f=100 Hz) ▬ ▬ ▬

method can be developed on the basis of the interesting luminescent properties of Eu(III) ions. We have carried out an exhaustive determination of ΔEp values at different scan rates finding a linear behavior between ΔEp and the square root of the scan rate for Eu(III) binary and ternary systems, which agrees very well with the theory for a typical quasireversible process. In fact, according to this theory, the kinetic parameter Ψ varies linearly with $\nu^{1/2}$, and ΔEp approaches linearity for small Ψ. Consequently, in this zone ΔEp should vary linearly with $\nu^{1/2}$. Because of the quasi-reversibility for the electrochemical reduction of the binary and ternary Eu(III) systems under investigation, it may be possible to study the kinetics of the electrode reaction. The separation of the peak potentials, ΔEp, should be a measure of the standard rate constant for the electron transfer. These ΔEp values were introduced in the working curve described by Nicholson [53] for obtaining the transfer parameter, Ψ, and then the standard heterogeneous charge-transfer rate constant (K_0) for the electron-transfer process can be calculated.

Spectral measurements for Eu(III) binary complexes with L1 and L2 and their interactions with DNA

UV and Fluorescence Measurements

Optimization of the Reaction Conditions Related to the Ternary Complex Formation

The coordination of Eu(III) to the methoxy derivative L1 is accompanied by a blue shift of the π- π* transition band of the ligand(λ=235 nm) whith enhancement of the peak located at λ=286 nm which may be attributed to n→π* band .

In the case of L2 the π- π* band located in the range (235–240 nm) is splitted into two peaks at λ_1=207 nm and λ_2=261 nm upon coordination with Eu(III).

The interaction of Eu(III)–L1 binary complex with CT-DNA in approximately 1:1 ratio doesn't exhibit any appreciable change in the band located at 210 nm while the second band at λ=284 nm is slightly enhanced upon interaction with CT- DNA as shown in Figs. 16 and 17.

The interaction of Eu(III)–L2 complex in the concentration range (3.72×10^{-4}-1.86×10^{-3} mol dm^{-3}) with CT- DNA (5.4×10^{-5} mol dm^{-3}) is shown in Fig. 18 where the UV spectra for the uncombined binary complex exhibits two absorption peaks at λ_1=209 nm and λ_2=262.30 nm. For the two concentrations of the complex 3×10^{-4} to 1×10^{-3} mol dm^{-3} , there is no appreciable shift in the absorption bands upon reaction with CT–DNA (in complex: DNA 6 to 20) while there is an enhancement in the molar absorptivity of the two peaks . Upon increasing the concentration of the complex from 1×10^{-3} to 1.8×10^{-3} mol dm^{-3} i.e complex : DNA ratio (20:33) there is also a noticeable enhancement in

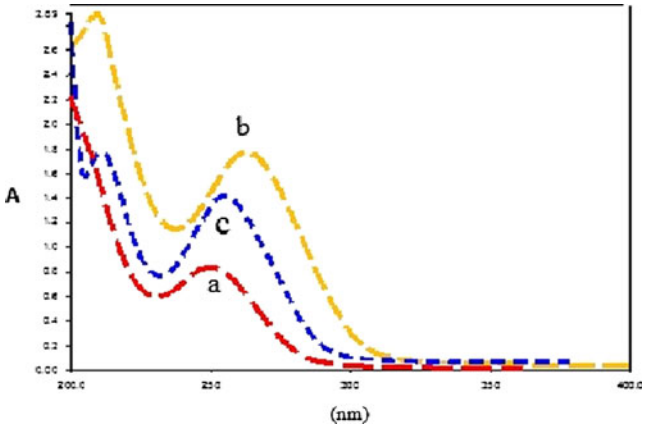

Fig. 16 UV absorption spectra for Eu(III)- (2-{[4-methyl benzoyl] oxy methyl }benzoic acid) complex with (CT–DNA(system in phosphate buffer pH7.00 at 25 °C. a- 5.4× 10^{-5} mol dm^{-3} free (CT–DNA). b- 3.72× 10^{-4} mol dm^{-3} Eu(III)- (2-{[4-methyl benzoyl] oxy methyl } benzoic acid). C- 3.72× 10^{-4} mol dm^{-3} Eu(III)- (2-{[4-methyl benzoyl] oxy methyl } benzoic acid)+5.4× 10^{-5} mol dm^{-3} free (CT–DNA)

molar absorptivity especially in the second absorption peak located at λ=260 nm . There is a clear perturbation in the absorption peaks where three peaks are obtained at λ_1=227, λ_2=247 and λ_3=269 nm with nearly the same molar absorptivity , upon interaction of the complex with CT-DNA in (34:1) complex : DNA ratio.

The interaction of Eu(III)-L2 with CT–DNA in approximately equimolar concentration is accompanied by lowering of the molar absorptivity of the peak located at λ= 207 nm .The band located at λ=261 nm is slightly lowered. In comparison to the UVspectra of CT–DNA , the characteristic band observed at λ=260 nm is enhanced upon interaction with both Eu(III)–L2 complex .The binary complex of Eu(III)-phloroglucinol exhibits two absorption

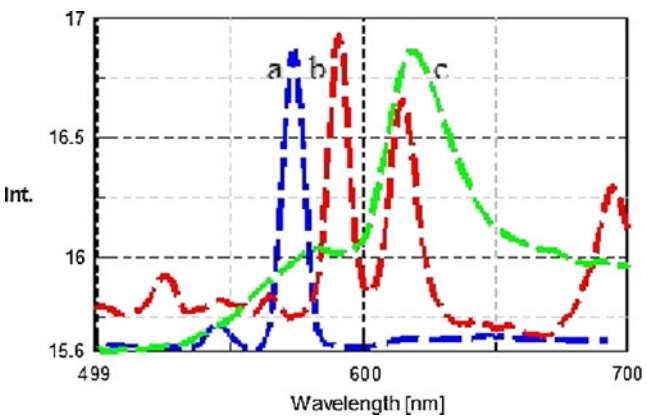

Fig. 17 Fluorescence spectra for Eu(III)—(2-{[4-methyl benzoyl] oxy methyl }benzoic acid) complex with (CT–DNA(system in phosphate buffer pH7.0 at 25 °C. a- 5.4× 10^{-5} mol dm^{-3} free (CT–DNA). b- 3.72× 10^{-4} mol dm^{-3} Eu(III)- (2-{[4-methyl benzoyl] oxy methyl } benzoic acid). C- 3.72× 10^{-4} mol dm^{-3} Eu(III)- (2-{[4-methyl benzoyl] oxy methyl } benzoic acid)+5.4× 10^{-5} mol dm^{-3} free (CT–DNA)

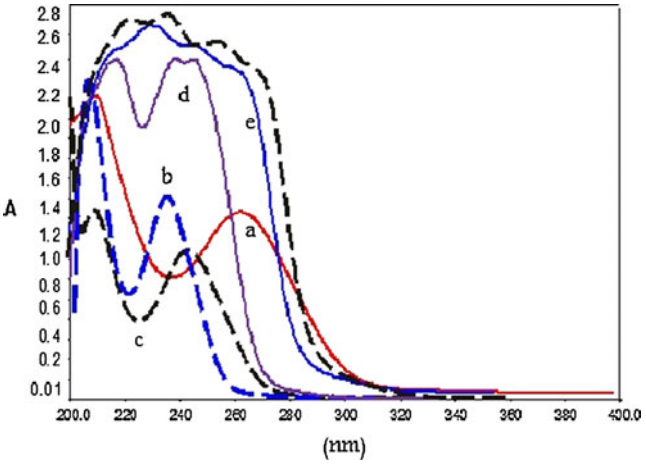

Fig. 18 Effect of concentration on Uv absorption spectra of Eu(III) (2-{[4-methyl benzoyl] oxy methyl } benzoic acid) complex with CT–DNA in phosphate buffer pH 7.0 at 25 °C . [CT–DNA]=5.4× 10^{-5} mol dm^{-3}. **a** free Eu(III)-L2 binary complex (3.75×10^{-4} mol dm^{-3}). **b** Eu(III)L2 complex-DNA (complex : DNA ratio=6.88 : 1). **c** Eu(III)L2 complex-DNA (complex : DNA ratio=13.70 : 1). **d** Eu(III)L2 complex-DNA (complex : DNA ratio=20.66 : 1). **e** Eu(III)L2 complex-DNA (complex : DNA ratio=27.55: 1). **f** Eu(III)L2 complex-DNA (complex : DNA ratio=34.44: 1)

bands at λ_1=203 and λ_2=262 nm and a small shoulder at λ =227 nm . The interaction of the complex with CT- DNA causes a dramatic decrease of the band observed at λ= 203 nm and a slight decrease of the third band located at λ =268 nm while the shoulder observed at λ=262 nm is slightly decreased.

Fluorescence spectra for the complex system Eu(III)-(2-{[4-methyl benzoyl] oxy methyl }benzoic acid) with (CT–DNA) in phosphate buffer pH 7.0 is given in Fig. 17.

The effect of concentration of CT- DNA on the fluorescence spectra of Eu(III)-(2-{[4-methyl benzoyl]

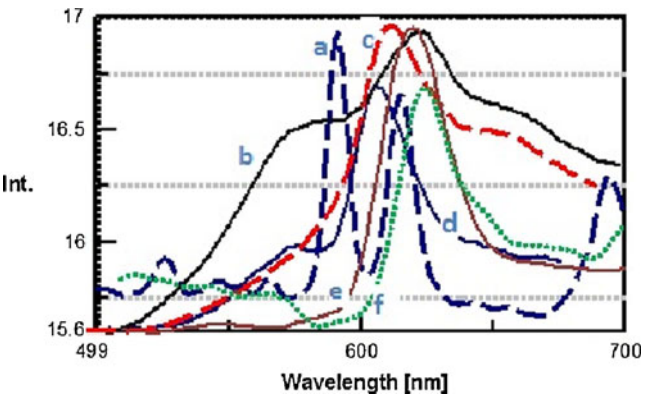

Fig. 19 Effect of concentration on fluorescence spectra of Eu(III) -(2-{[4-methyl benzoyl] oxy methyl } benzoic acid) complex with CT- DNA in phosphate buffer pH 7.0 at 25 °C . [CT- DNA]=5.4× 10^{-5} mol dm^{-3}. **a** Eu(III)-L2 binary complex (3.75×10^{-4} mol dm^{-3}). **b** Eu(III)-L2-CT–DNA (complex: DNA ratio=6.88 : 1). **c** Eu(III)-L2-CT–DNA (complex : DNA ratio=13.70 : 1). **d** Eu(III)-L2- CT–DNA (complex : DNA ratio =20.66 : 1). **e** Eu(III)-L2- CT–DNA (complex : DNA ratio=27.55 : 1). **f** Eu(III)-L2- CT–DNA (complex : DNA ratio=34.44 : 1)

Table 6 Analytical data for Eu(III) – L2 solid complex

Complex	Formula	H%		C%		M.P °C
		Calc	Found	Calc	Found	
Eu(III)-L2	$Eu(C_{15}H_{12}O_3)_2Cl_2.8H_2O$	42.50	40.68	4.72	3.67	142-145

oxy methyl } benzoic acid) complex in phosphate buffer pH 7.0 is shown in Fig. 19 .

The fluorescence spectra for a solution of 5.4×10^{-5} mol dm^{-3} of CT- DNA has an emission peak at λ= 540 nm with an intensity of 2.60 . The Eu(III) – L2 complex has two emission bands at λ_1=590 nm and λ_2= 618 nm which may be attributed to $^5D_o\rightarrow{}^7F_1$ and $^5D_o\rightarrow{}^7F_2$ transitions . Upon interaction of Eu(III) –L1 with CT-DNA only one emission band is observed at λ=617 nm which is due to $^5D_o\rightarrow{}^7F_2$ transition, while the two characteristic bands for Eu(III) –L1 disappeared .For the reaction of Eu(III) –L2 with CT- DNA two emission bands are observed at λ_1=618 nm and λ2=654 nm which could be assigned to $^5D_o\rightarrow{}^7F_2$ and $^5D_o\rightarrow{}^7F_3$, respectively .

It is clearly observed that the emission band at λ= 618 nm is enhanced slightly upon interaction with CT-DNA and a new transition band is observed at λ=654 nm . Upon interaction of Eu(III)-phloroglucinol complex with CT- DNA the three emission bands located at λ_1=588 nm , λ_2=617 nm and λ_3=647 nm which could be attributed to $^5D_4\rightarrow{}^7F_1$, $^5D_4\rightarrow{}^7F_2$ and $^5D_4\rightarrow{}^7F_3$ transitions are greatly enhanced . This observation could be attaributed to a specific strong binding manner of Eu(III)-phloroglucinol complex with CT- DNA . The enhancements in the emission intensity of Eu(III)-phloroglucinol with increasing CT–DNA concentration has been observed. In the absence of CT–DNA it emits weak luminescence in phosphate buffer (pH=7.0). Upon addition of CT- DNA the emission intensity of the complex grows steadily. Although the emission enhancement could not be regarded as a criterion for binding mode, they are related to the extent to which the complex gets into a hydrophobic environment inside CT-DNA and avoids the complex effect of solvent water molecules. Complex formation between energy donor and acceptor,as in our present case of the interaction between complex with CT–DNA, guarantees a more efficient energy transfer which results in enhancement of Eu(III)-phloroglucinol complexes.Visicosity measurements confirmed the formation of CT–DNA- Eu(III)-phloroglucinol complex.

Characterization of Eu(III)–L2 Solid Complex

The synthesized complexe Eu(III)–L2 is characterized and the analytical data are collected in Table 6.

As depicted in Table 6, the solid complex is crystallized in metal: ligand ratio 1:2, as obtained from the elemental analysis and the estimation of the metal content in the solid complex. The formed complex is of electrolytic nature as confirmed by the formation of white precipitate of two moles of AgCl upon reacting with $AgNO_3$.

The FTIR spectra for the synthesized L2 and the corresponding Eu(III)-L2 complex is depicted in Fig. 20. The stretching frequency of the COO^- group occurs at 1668 cm^{-1} is shifted upon coordination to the Eu(III) metal ions indicating that the negative oxygen is the major coordination center of binding with the lanthanide metal ions. The broad band observed at 3320 cm^{-1} could be attributed to the stretching frequency of coordinated water molecules to the central metal ions.

Conclusion

Two new ligands derived from phloroglucinol 2-{[(4-methoxy benzoyl) oxy] } methyl benzoic acid[L1] and 2-{[(4-methyl benzoyl)oxy] methyl} benzoic acid[L2] were synthesized and characterized. The solid complex Eu (III)-L2 has been synthesised and characterized by elemental analysis ,UV and IR spectra.The DTA and IR studies indicate the mode of interaction of Eu(III) ions with the investigated ligands during the binary complex formation. The electrochemical reactions of Eu(III) with the two synthesized ligands has been investigated in I=0.1 mol dm^{-3} p-toluene sulfonate by cyclic voltammetry and square wave voltammetry on a glassy carbon electrode. Voltammetric data for Eu(III)–nucleotide -L1 or L2 in 0.1 mol dm^{-3} p-toluene sulfonic acid at 25 °C have been calculated. In the present

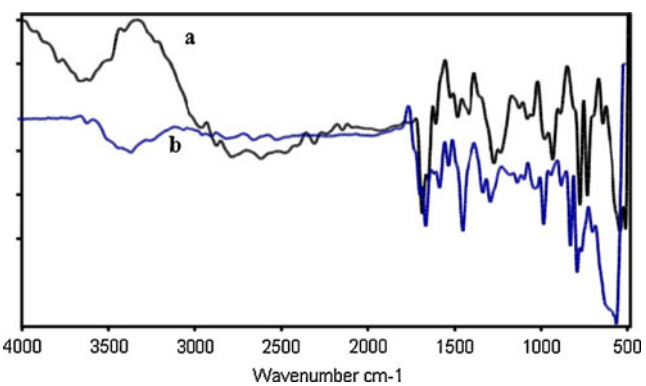

Fig. 20 FTIR spectra for Eu(III)-(2-{[4-methyl benzoyl] oxy methyl } benzoic acid) complex

study,the reaction of Eu (III)–L1 and Eu (III)–L2 binary complexes with nucleotide 5′-AMP , 5′-ADP ,5′-ATP , 5′-GMP , 5′-IMP , and 5′-CMP has been investigated using UV, fluorescence and electrochemical methods. The interaction of the Eu(III)–L1 or L2 solid complexes with calf-thymus DNA has been investigated by fluorescence and electrochemical methods including cyclic voltammetery(CV) ,differential pulse polarography (DPP) and square wave voltammetry (SWV) on a glassy carbon electrode. In this work, we observed the interesting phenomenon that if CT–DNA was added into Eu (III)-phloroglucinol derivatives solutions, the CT–DNA–Eu (III)-phloroglucinol derivatives systems can produce the strong fluorescence emission. By taking advantage of this phenomenon, a new strategy for CT–DNA hybridization can be suggested using Eu (III)-phloroglucinol derivatives as fluorescence probe. Furthermore, this label-free method for CT–DNA hybridization detection can avoid the laborious labeling or modifying steps, which can make the process simple, rapid, and low in cost; the hybridization and detection are performed in homogeneous solution without steric constraints.

The results indicate the possibility of *DNA and* nucleotide 5′-AMP , 5′-ADP ,5′-ATP , 5′- GMP , 5′-IMP , and 5′-CMP quantification using the new Eu (III)–L1 and Eu (III)–L2 binary complexes synthesized during this study.

References

1. Wisespongpand P, Kuniyoshi M (2003) Bioactive phloroglucinols from the brown alga *Zonaria diesingiana*. J Appl Phycol 15:225–228
2. Broadbent D, Mabelis RP, Spencer H (1976) C-acetylphloroglucinols from *Pseudomonas fluorescens*. Phytochemistry 15(11):1785
3. Mathegka ADM, Meyer JJM, Horn MM, Drewes SE (2000) An acylated phloroglucinol with antimicrobial properties from *Helichrysum caespititium*. Phytochemistry 53:93–96
4. Meyer JJ, Lall N, Mathegka ADM (2002) Extraction of antibacterial compounds from Combretum microphyllum (Combretaceae). S Afr J Bot 68:90–93
5. Mathekga ADM (2001) Antimicrobial activity of Helichrysum species and the isolation of a new phloroglucinol from *Helichrysum caespititium*. Doctoral thesis at the University of Pretoria.
6. Yamaki M, Miwa M, Ishiguro KS, Takagi S (1994) Antimicrobial activity of naturally occurring and synthetic phloroglucinols against *Staphylococcus aure*. Phytother Res 8:112–114
7. Rocha L, Marston A, Potterat O, Kaplan MAC, Hostettmann K (1996) More phloroglucinols from *Hypericum brasiliense*. Phytochemistry 42:185–188
8. Heilmann J, Winkelmann K, Sticher O (2003) Studies on the antioxidative activity of phloroglucinol derivatives isolated from *Hypericum* species. Planta Med 69:202–206
9. Tziveleka L, Vagias C, Roussis V (2003) Natural products with anti-HIV activity from marine organisms. Curr Top Med Chem 3:1512–1535
10. Singh IP, Bharate SB (2006) Phloroglucinol compounds of natural origin. Nat Prod Rep 23:558–591
11. Verotta L (2003) Are acylphloroglucinols lead structures for the treatment of neurodegenerative diseases? Phytochem Rev 1:389–407
12. Mandix K, Colding A, Elming K, Sunesen L, Shim I (1993) Ab initio investigation of phloroglucinol. Int J Quant Chem 46:159–170
13. Spoliti M, Bencivenni L, Quirante JJ, Ramondo F (1997) Molecular conformations and harmonic force field of 1,3,5-benzenetriol molecule from ab initio and density functional theory investigations. J Mol Struct (Theochem) 390:139–148
14. National Hygienic Standards for the Usage of Food Additives, GB (1996) Standardization Administration of China: pp 2760–1996
15. Jayabalan M, Thomas V, Rajesh PN (2001) Polypropylene fumarate/phloroglucinol triglycidyl methacrylate blend for use as partially biodegradable orthopaedic cement. Biomaterials 22:2749–2757
16. Higuchi K, Motomizu S (1999) Flow-injection spectrophotometric determination of nitrite and nitrate in biological samples. Anal Sci 15:1
17. Pesez M, Bartos J (1974) Colorimetric and fluorimetric methods of analysis. Dekker, New York, p 109
18. Buono-core GE, Marciniak B, Li H (1990) Coord Chem Rev 99:55–87
19. Wu WN, Tang N, Yan L (2008) J Fluoresc 18:101–107
20. Wang QM, Yan B (2004) J Mater Chem 14:2450
21. Edward A, Chu TY, Claude C, Sokolik I, Okamoto Y, Dorsinville R (1997) Synth Met 84:433–434
22. Kido J, Nagai K, Okamoto Y (1993) J Alloys Compd 192:30
23. Yu JB, Zhou L, Zhang HJ, Zheng YX, Li HR, Deng RP, Peng ZP, Li ZF (2005) Inorg Chem 44:1611
24. Kukhta A, Kolesnik E, Grabchev I (2006) J Fluoresc 16:375–378
25. Meares CF, Wensel TG (1984) Acc Chem Res 17:202
26. Wu FB, Zhang C (2002) Anal Biochem 311:57–67
27. Nishioka T, Yuan J, Yamamoto Y, Sumitomo K, Wang Z, Hashino K, Hosoya C, Ikawa K, Wang G, Matsumoto K (2006) Inorg Chem 45:4088–4096
28. Scott LK, Horrocks WD (1992) J Inorg Biochem 46:193
29. Niyama E, Brito HF, Cremona M, Teotonio EES, Reyes R, Birto GES, Felinto MCFC (2005) Spectrochim Acta Part A 61:2643–2649
30. Lehn JM (1990) Angew Chem Int Ed Engl 29:1304–1319
31. An BL, Gong ML, Li MX, Zhang JM, Cheng ZX (2005) J Fluoresc 15:613–617
32. Lv Y, Zhang J, Cao W, Juan JC, Zhang F, Xu Z (2007) J Photochem Photobiol A 188:155–160
33. Meshkova SB (2000) J Fluoresc 10:333–337
34. Wood KC, Little SR, Langer R, Hammond PT (2005) A family of hierarchically self-assembling linear-dendritic hybrid polymers for highly efficient targeted gene delivery. Angew Chem Int Ed 44:6704–6708
35. Sassolas A, Leca-Bouvier BD, Blum LJ (2008) DNA biosensors and microarrays. Chem Rev 108:109–139
36. Epstein JR, Biran I, Walt DR (2002) Fluorescence-based nucleic acid detection and microarrays. Anal Chim Acta 469:3–36
37. Zheng W, He L (2009) Label-free, real-time multiplexed DNA detection using fluorescent conjugated polymers. J Am Chem Soc 131:3432–3433
38. Yang R, Tang Z, Yan J, Kang H, Kim Y, Zhu Z, Tan W (2008) Noncovalent assembly of carbon nanotubes and single-stranded DNA: an effective sensing platform for probing piomolecular interactions. Anal Chem 80:7408–7413
39. Liu Y, Wang Y, Jin J, Wang H, Yang R, Tan W (2009) Fluorescent assay of DNA hybridization with label-free molecular switch: reducing background-signal and improving specificity by using carbon nanotubes. Chem Commun 665–667.
40. Ws KN, O'Connell M, Wisdom JA, Dai HJ (2005) Carbon nanotubes as multifunctional biological transporters and nearinfrared agents for selective cancer cell destruction. Proc Natl Acad Sci USA 102:11600–11605

41. Tyagi S, Kramer FR (1996) Molecular beacons: probes that fluoresce upon hybridization. Nat Biotechnol 14:303–308
42. Azab HA, Anwar ZM, Ahmed RG (2010) Pyrimidine and purine mononucleotides recognition by trivalent lanthanide complexes with N-acetyl amino acids. J Chem Eng Data 55(1):459–475
43. Azab HA, El-Korashy SA, Anwar ZM, Hussein BHM, Khairy GM (2010) Synthesis and Fluorescence properties of Eu-anthracene-9-carboxylic acid towards N-acetyl amino acids and nucleotides in different solvents. Spectrochim Acta A Mol Biomol Spectrosc 75:21–27
44. Azab HA, Abd El-Gawad II, Kamel RM (2009) Ternary complexes formed by the fluorescent probe Eu (III)-9-anthracene carboxylic acid with pyrimidine and purine nucleobases. J Chem Eng Data 54:3069–3078
45. Azab HA, El-Korashy SA, Anwar ZM, Hussein BHM, Khairy GM (2010) Eu(lll)-anthracene-9-carboxylic acid as a responsive luminescent bioprobe and its electroanalytical Interactions with N-acetyl amino acids, nucleotides and DNA. J Chem Eng Data 55:3130–3141
46. Azab HA, Abd El-Gawad II, Kamel RM (2009) Ternary complexes formed by the fluorescent probe Eu (III)-9-anthracene carboxylic acid with pyrimidine and purine nucleobases. J Chem Eng Data 54:3069–3078
47. Filip W, Mojmir S, Li AX, Azab HA, Bartha R, Hudson RHE (2007) A robust and convergent synthesis of dipeptides-DOTAM conjugates as chelators for lanthanide ions: new PARACEST MRI agents. Bioconjug Chem 18(5):1625–1636
48. Orabi AS, Azab HA, ElDeghidy FS, Said H (2010) Ternary complexes of La(III), Ce(III), Pr(III) or Er(III) with adenosine 5'-mono,5'-di, and 5'-triphosphate as primary ligands and some biologically important zwitterionic buffers as secondary ligands. J Solution Chem 39:319–334
49. Azab HA, Al-Deyab SS, Anwar ZM, Gharib RA (2011) Fluorescence and electrochemical probing of N-acetylamino acids, nucleotides and DNA by Eu(lll) -bathophenanthroline complex. J Chem Eng Data 56(4):833–849
50. Azab HA, Al-Deyab SS, Anwar ZM, Kamel RM (2011) Potentiometric, electrochemical and fluorescence study of the coordination properties of the monomeric and dimeric complexes of Eu(lll) with nucleobases and PIPES. J Chem Eng Data 56:1960–1969
51. Azab HA, Al-Deyab SS, Anwar ZM, Abd El-Gawad II, Kamel RM (2011) Comparison of the coordination tendency of amino acids, Nucleobases or mononucleotides towards the monomeric and dimeric lanthanide complexes with biologically important compounds. J Chem Eng Data 56:2613–2625
52. Suh D, Chaires JB (1995) Criteria for the mode of binding of DNA binding agents. Bioorg Med Chem 3:723–728
53. Nicholson RS (1965) Theory and application of cyclic voltammetry for measurement of electrode reaction kinetics. Anal Chem 37:135